Cumhuriyet Sci. J., 47(3) (2026) 557-565
DOI: 10.17776/csj.1833921

Cumhuriyet Science Journal

http://csj.cumhuriyet.edu.tr Founded: 2002 ISSN: 2587-2680 e-ISSN: 2587-246X Publisher: Sivas Cumhuriyet University

Structural, Morphological, and Photocatalytic Comparison of TiO_2 Thin Films Deposited by RF Magnetron Sputtering at Room Temperature and 300 °C

Ahmet Çetin [1,a,*], Mehmet Şimşir [1,b], Ebru Şenadım Tüzemen[2,3,c], Ali Özer [1,4,d]

[1] *Department of Metallurgical and Materials Engineering, Faculty of Engineering, Sivas Cumhuriyet University, 58140 Sivas, Türkiye.*
[2] *Department of Physics, Faculty of Science, Sivas Cumhuriyet University, 58140 Sivas, Türkiye.*
[3] *Sivas Cumhuriyet University Nanophotonics Application and Research Center-CÜNAM, 58140 Sivas, Türkiye.*
[4] *Geoship SPC, Material Science Laboratory, Grass Valley, CA, USA.*
**Corresponding author e-mail address: ctnahmet@gmail.com*

Research Article

History
Received: 01.12.2025
Accepted: 04.05.2026

ABSTRACT

In this study, TiO_2 thin films were deposited onto glass substrates at room temperature and at a moderate substrate temperature of 300 °C by RF magnetron sputtering, and their structural, morphological, chemical, and photocatalytic properties were comparatively investigated. XRD analysis revealed that the film deposited at room temperature was fully amorphous, whereas the film deposited at 300 °C exhibited weak anatase reflections superimposed on an amorphous background, indicating the onset of crystallization. Cross-sectional SEM images confirmed the formation of a homogeneous film with an approximate thickness of 330 nm, while surface SEM observations showed a denser and more developed surface morphology for the film grown at elevated temperature. AFM measurements demonstrated that the film deposited at 300 °C possessed a markedly rougher granular surface. FTIR spectra revealed the characteristic Ti–O–Ti vibrational bands, confirming the formation of the TiO_2 network structure. Photocatalytic experiments showed that the TiO_2 film deposited at 300 °C achieved approximately 74% degradation of methylene blue under UV-A irradiation after 9 h, exhibiting significantly higher activity than the room-temperature film. This enhanced performance is attributed to the combined effect of incipient anatase formation and increased surface roughness. Overall, the results demonstrate that low-temperature structural evolution strongly influences the photocatalytic response of sputtered TiO_2 thin films, and that appreciable photocatalytic performance can be achieved at 300 °C without a separate post-deposition annealing step.

This article is licensed under a Creative Commons Attribution-NonCommercial 4.0 International License (CC BY-NC 4.0)

Keywords: *Photocatalytic Activity, RF Magnetron Sputtering, Substrate Temperature, Surface Morphology, TiO_2 Thin Films.*

[a] 0009-0003-6991-656X
[b] 0000-0002-8895-7821
[c] 0000-0001-9166-7422
[d] 0000-0002-4207-8207

1. Introduction

The contamination of water resources with synthetic dyes and persistent organic pollutants has become a major global environmental concern due to rapid population growth and expanding industrial activities, thereby increasing the demand for efficient oxidation-based remediation strategies [1,2]. The inadequacy of conventional treatment methods against such compounds has increased interest in Advanced Oxidation Processes (AOPs), which are capable of generating highly reactive oxidizing species [1]. Among various AOPs, heterogeneous photocatalysis is considered one of the most promising techniques because it can directly utilize solar energy, operates without the need for chemical additives, and can promote the mineralization of organic pollutants into simpler end products [1-3]. The concept of photocatalysis originates from the pioneering work of Fujishima and Honda in 1972 on TiO_2 electrodes, which is widely regarded as a milestone in the development of the field [4].

TiO_2 is a widely used semiconductor in photocatalytic applications due to its bandgap energy of approximately 3.2 eV, high chemical stability, low toxicity, and cost-effectiveness [3,5]. However, its activity is limited mainly to the UV region, and the rapid recombination of photogenerated charge carriers remains a major drawback restricting its efficiency [3,5]. Although TiO_2 powders offer high surface area, issues such as particle agglomeration in solution, difficulty in recovery, and the risk of secondary pollution make thin-film configurations more attractive for practical applications, including photocatalytic coatings, self-cleaning surfaces, antibacterial interfaces, and water-treatment systems [2,3,6].

TiO_2 thin films can be fabricated through various techniques such as sol–gel, CVD, ALD, and PVD methods [4,5], among which reactive magnetron sputtering stands out owing to its high film uniformity, strong substrate adhesion, and good compatibility with large-area coating technologies [5,7]. In addition, sputter deposition enables relatively precise control over film thickness, microstructure, defect chemistry, and stoichiometry, all of which can strongly influence photocatalytic behavior

[5,7]. Recent studies have shown that substrate temperature is one of the key parameters in sputter deposition, directly influencing the crystalline phase evolution, surface morphology, roughness, defect structure, charge carrier dynamics, and ultimately the photocatalytic performance of the resulting films [5,8,9].

Photocatalytic activity can vary depending on factors such as crystal phase composition (anatase, rutile, or amorphous), structural disorder, defect states, surface roughness, and substrate-related effects in supported thin-film systems [3,5,10,11]. Despite extensive research on TiO_2 thin films, the relationship between low-temperature structural evolution and photocatalytic performance is still not sufficiently clarified for RF-sputtered films deposited directly on widely used soda–lime glass substrates. In particular, it remains important to determine whether appreciable photocatalytic activity can be achieved at a moderate deposition temperature without a separate post-deposition annealing step. This study aims to systematically elucidate the relationship between structural evolution and photocatalytic performance in TiO_2 thin films deposited at room temperature and at a relatively low substrate temperature of 300 °C by RF magnetron sputtering on widely used and cost-effective soda–lime glass substrates. The thin films were characterized using XRD, SEM/EDX, AFM, FTIR, and UV–Vis spectrophotometry, while photocatalytic activity was evaluated through the degradation kinetics of methylene blue under UV-A irradiation. The present study demonstrates that deposition at 300 °C can induce the onset of anatase crystallization, increase surface roughness, and significantly improve the photocatalytic activity of sputtered TiO_2 thin films without an additional annealing step. These findings provide a clearer understanding of the role of substrate temperature in the structural and functional evolution of TiO_2 thin films.

2. Materials and Methods

2.1 Deposition of Thin Films

In this study, TiO_2 thin films were deposited onto glass substrates using the RF magnetron sputtering technique. The coating processes were carried out in a NANOVAK NVTS-400 thermal–sputter combined system. A high-purity (99.999%) TiO_2 target was used, and the films were deposited at room temperature and at a substrate temperature of 300 °C under the following conditions: a substrate rotation speed of 10 rpm, RF power of 110 W, deposition rate of 0.4–0.6 Å s^{-1}, and a working pressure of 7 mTorr. Except for the substrate temperature, the deposition parameters were kept constant for both samples. Prior to deposition, the glass substrates were subjected to a standard cleaning procedure to minimize surface contamination, which involved sequential ultrasonic cleaning in acetone, ethanol, and deionized water. After cleaning, the substrates were dried under ambient conditions to ensure compatibility with the deposition process.

2.2 Characterization Methods

The phase composition of the TiO_2 thin films was determined by X-ray diffraction (XRD) using a PANalytical EMPYREAN diffractometer with Cu–Kα radiation (λ = 1.5406 Å). XRD data were collected in Bragg–Brentano mode over a 2θ interval of 20°–80°. The surface morphology and elemental features of the samples were investigated by SEM/EDX using a TESCAN Mira 3 microscope. Surface topography and roughness measurements were carried out with a Park Systems XE7 atomic force microscope operating in contact mode. The chemical bonding characteristics of the films were further examined using a Bruker Tensor II Fourier Transform Infrared Spectrometer (FTIR).

2.3 Photocatalytic Tests

The photocatalytic activity of the TiO_2 thin films was evaluated based on the degradation of methylene blue (MB) dye in aqueous solution. Photocatalytic experiments were carried out in a cylindrical UV-A photoreactor system equipped with eight 8 W fluorescent lamps (Philips Actinic BL, λ ≤ 365 nm). The reaction medium consisted of 70 mL of MB solution with an initial concentration of 2.5 mg L^{-1} (pH = 7.9). As part of the experimental procedure, prior to activating the light source, the system was stirred under dark conditions for 30 min to establish adsorption–desorption equilibrium. Subsequently, UV-A irradiation was initiated, and 3 mL aliquots were collected at predetermined time intervals. Changes in MB concentration were monitored by measuring the characteristic absorbance at 664 nm using a Thermo Scientific Evolution 201/220 UV–Vis spectrophotometer. The degradation efficiency (η, %) was calculated using $\eta\ (\%) = [(C_0 - C_t)/C_0] \times 100$, where C_0 is the initial MB concentration and Ct is the concentration at irradiation time t. Additionally, the reaction kinetics were evaluated using a pseudo-first-order kinetic model expressed as $-\ln(C_t/C_0) = k \cdot t$ [8], where t is the irradiation time (min) and k is the pseudo-first-order rate constant (min^{-1}).

3. Results

3.1 XRD Results

According to the diffraction patterns presented in Figure 1, the TiO_2 thin film deposited at room temperature exhibits no discernible diffraction peaks.

.

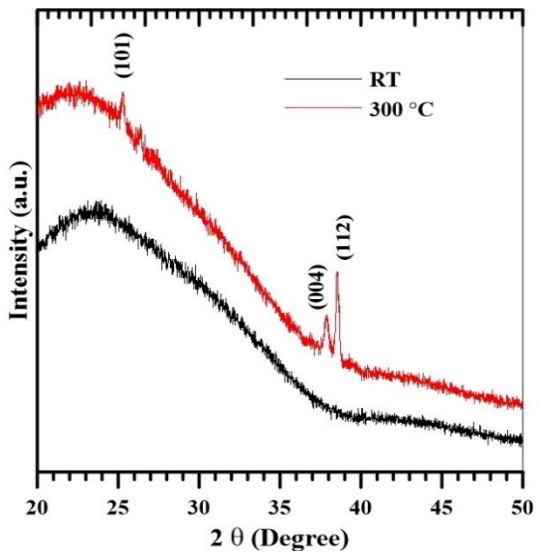

Figure 1. XRD patterns of TiO_2 thin films deposited at room temperature and 300 °C

The film displays a broad scattering band in the range of 20–35°, without any reflections corresponding to the characteristic anatase (101) or rutile (110) phases. This behavior indicates the formation of an amorphous structure, which is commonly reported in the literature for TiO_2 deposited at low temperatures due to limited atomic diffusion [12]. The amorphous character, typically observed in films produced by low-temperature techniques such as RF sputtering and related thin-film deposition routes, is generally manifested through broad hump-like scattering features [13-14].

In contrast, the TiO_2 film deposited at a substrate temperature of 300 °C exhibits low-intensity yet distinguishable anatase peaks superimposed on the amorphous background. Reflections corresponding to the anatase phase are identified at 2θ ≈ 25.3°, 37.89°, and 38.53°, assigned respectively to the (101), (004), and (112) planes. These positions are consistent with the JCPDS card No. 21-1272, and the low peak intensities indicate that crystallization is still at an initial stage. Recent studies similarly report that TiO_2 films deposited at low substrate temperatures remain amorphous or weakly crystalline, while weak anatase peaks begin to appear with increasing substrate temperature [8-9].

For crystallite size evaluation, the anatase (101) and (112) peaks—which exhibit higher signal-to-noise ratios—were modeled using a Gaussian fitting function, yielding FWHM values of 0.259° and 0.227°, respectively. Using the Scherrer equation, crystallite sizes were calculated as 31.5 nm for the (101) plane and 37.0 nm for the (112) plane. These results confirm that limited nucleation occurs at 300 °C and that crystallinity begins to develop in a controlled manner. The Scherrer equation used for crystallite size calculations is expressed as:

$$D = \frac{K\lambda}{\beta cos\theta}$$

Where K = 0.9, λ = 0.15406 nm (Cu–Kα), β is the FWHM (in radians), and θ is the Bragg angle [15].

3.2 SEM-EDX and AFM Results

As shown in Figure 2(a), the cross-sectional morphology of the TiO_2 film deposited at room temperature reveals the formation of a compact and continuous layer with a thickness of approximately 338 ± 10 nm.

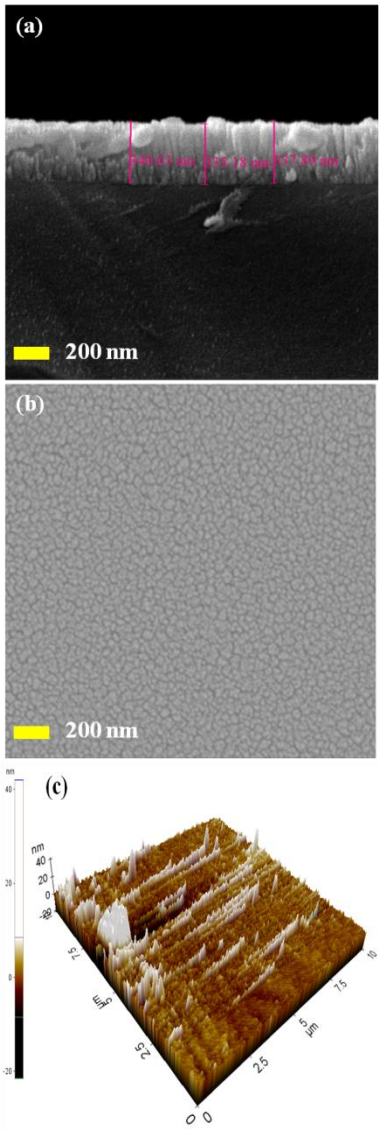

Figure 2. (a) Cross-sectional SEM image, (b) surface SEM morphology, (c) AFM surface topography of the TiO_2 film deposited at room temperature.

The surface SEM image in Figure 2(b) displays a smooth and homogeneous surface texture, lacking distinct grain boundaries. This compact and featureless morphology corresponds well with the low crystallinity commonly reported for amorphous TiO_2 films produced at low temperatures [12-13,16]. The AFM surface topography in Figure 2(c) shows slight micrometer-scale undulations and reveals an RMS roughness of 4.306 nm. This value is typical for sputtered TiO_2 films deposited at room temperature and indicates an irregular, low-roughness topography rather than ordered crystalline surface islands. Such a low roughness also suggests a limited effective surface development at the film/solution

interface. Taken together, these findings suggest that the TiO_2 film deposited at room temperature exhibits an amorphous or low-crystalline character due to limited atomic diffusion [12-13].

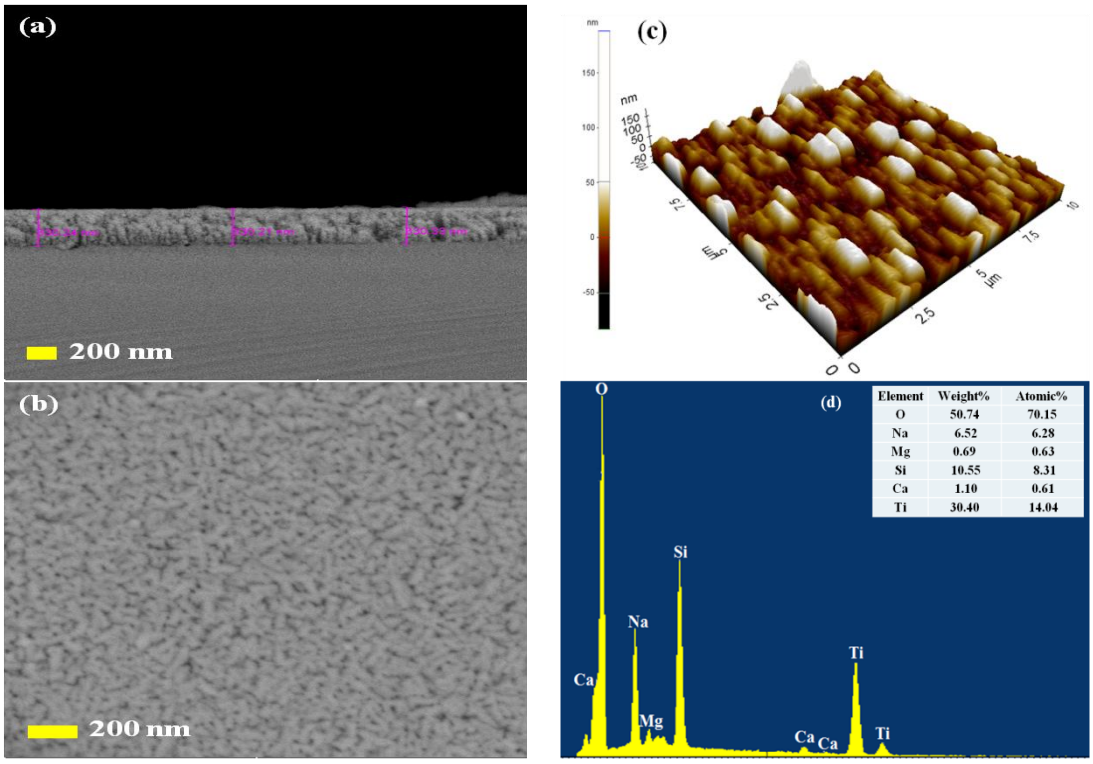

Figure 3. (a) Cross-sectional SEM image, (b) surface SEM morphology, (c) AFM surface topography of the TiO_2 film deposited at 300 °C, (d) SEM–EDX spectrum of the TiO_2 film deposited at 300 °C

The cross-sectional image shown in Figure 3(a) demonstrates that the TiO_2 film deposited at a substrate temperature of 300 °C has a thickness of approximately 330 ± 10 nm and exhibits a compact columnar microstructure extending from the substrate toward the surface. The limited spacing between the columns indicates that the film possesses high density and good structural continuity. Since the thicknesses of the RT and 300 °C films are very similar, the main effect of substrate temperature in the present study is associated primarily with structural and morphological evolution rather than with film thickness.

The surface SEM image in Figure 3(b) presents a granular morphology composed of fine nanoclusters, which is associated with the early surface evolution linked to the onset of limited crystallization in amorphous TiO_2 around 250–300 °C. The low-intensity anatase peak observed in the XRD pattern of this study supports this initial crystallization process [17].

The SEM-EDX spectrum shown in Figure 3(d) reveals distinct peaks corresponding to Ti and O, consistent with the presence of the TiO_2 coating, along with Na, Si, Ca, and Mg originating from the soda–lime glass substrate. The semi-quantitative EDX results indicate weight percentages of 50.74% O, 30.40% Ti, 10.55% Si, 6.52% Na, 1.10% Ca, and 0.69% Mg, corresponding to atomic percentages of 70.15% O, 14.04% Ti, 8.31% Si, 6.28% Na, 0.61% Ca, and 0.63% Mg. The combined contribution of the substrate-derived elements (Na, Si, Ca, and Mg) reaches 15.83 at%, indicating a non-negligible substrate/interfacial contribution within the analyzed volume. Considering the micrometer-scale interaction volume of EDX in thin-film/substrate systems, these substrate-derived elemental contributions are expected and should not be interpreted as a direct quantitative representation of the intrinsic TiO_2 film composition. The AFM surface topography in Figure 3(c) reveals a three-dimensional surface composed of nanometric protrusions and depressions, with an RMS roughness of 26.03 nm. This moderately high roughness is consistent with the granular morphology observed in SEM. Compared with the RT film, the RMS roughness increased by approximately six times, confirming a pronounced temperature-induced surface development. Overall, the TiO_2 film deposited at 300 °C represents an early stage in the transition from an amorphous structure to a crystalline anatase phase, characterized by columnar internal structure, granular surface morphology, increased roughness, and the appearance of weak anatase reflections in XRD.

3.3 FTIR Results

The FTIR spectra presented in Figure 4 show the fundamental vibrational bands of the reference glass substrate, and the TiO_2 films deposited at room temperature and at 300 °C.

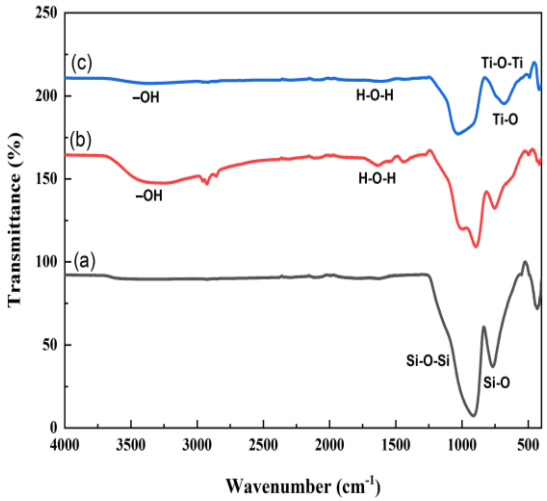

Figure 4. FTIR spectra of (a) reference glass substrate, (b) TiO_2 film deposited at room temperature, (c) TiO_2 film deposited at 300 °C

In the spectrum of the bare glass substrate, the dominant Si–O–Si stretching mode observed around 1100–1000 cm^{-1} and the Si–O bending vibrations located within the 800–450 cm^{-1} region represent the characteristic bands of soda–lime glass, serving as a reference for distinguishing film-related signals [18].

For the TiO_2 film deposited at room temperature, the broad and low-intensity band observed within the 1000–500 cm^{-1} range indicates that distinct Ti–O or Ti–O–Ti vibrational modes are not clearly formed, suggesting that the film possesses an amorphous Ti–O network structure. The –OH stretching vibration around 3300–3500 cm^{-1} and the H–O–H bending mode around 1630–1650 cm^{-1} correspond to surface-adsorbed water molecules and hydroxyl groups [19].

In the film deposited at 300 °C, these vibrational bands become sharper and more distinguishable in the same wavenumber region. In particular, the emergence of the Ti–O stretching mode near ≈670–700 cm^{-1} and the Ti–O–Ti bridging vibrations in the ≈520–550 cm^{-1} range indicates a higher degree of structural ordering in the film deposited at 300 °C and is consistent with the onset of crystallization suggested by the XRD results [19–20]. Furthermore, the reduced intensities of the –OH and H–O–H bands are attributed to the desorption of surface water and the development of a more stabilized Ti–O bonding structure with increasing temperature.

Overall, the FTIR findings indicate that the film deposited at room temperature retains a more disordered Ti–O structure, whereas the 300 °C film exhibits a more organized Ti–O/Ti–O–Ti bonding structure. These observations are consistent with the weak anatase-related features observed in XRD and with the temperature-induced structural evolution revealed by the SEM and AFM analyses.

3.4 Photocatalytic Results

The photocatalytic degradation of methylene blue (MB, 2.5 mg L^{-1}) by the TiO_2 film deposited at room temperature is presented in Figure 5. Under UV-A irradiation, the film achieved only 26% degradation after 360 min, and the pseudo–first–order kinetic model yielded a rate constant of k = 0.0006 min^{-1}, indicating poor photocatalytic activity. The low degradation performance is consistent with the amorphous nature of the RT–TiO_2 film, as amorphous structures exhibit limited surface activity and generally lower photocatalytic efficiency, as widely reported in the literature [21–24]. The low degradation efficiency obtained in this study is therefore coherent with the limited crystallization and reduced surface activity of the amorphous TiO_2 film. For a more reliable comparison between the two films, the photocatalytic behaviour was also evaluated using the pseudo-first-order rate constant.

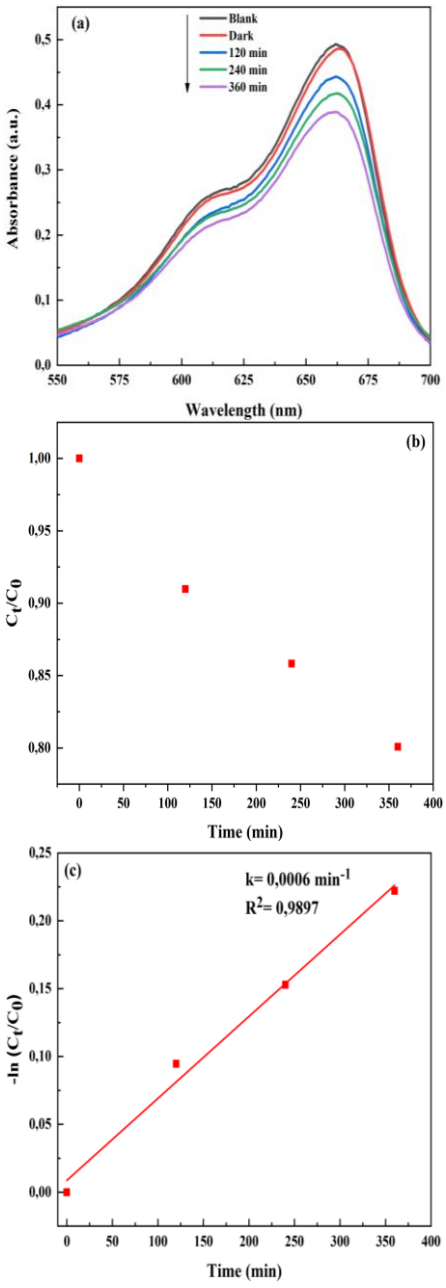

Figure 5. Photocatalytic activity of the TiO_2 film deposited at room temperature: (a) absorbance variation, (b) C_t/C_o degradation curve, (c) $-\ln(C_t/C_o)$ pseudo-first-order kinetic plot

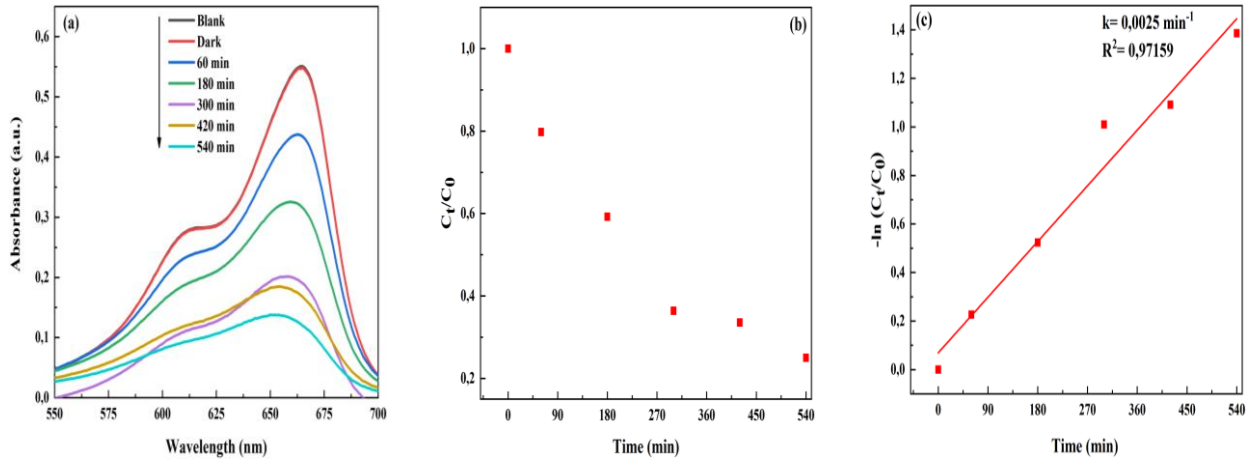

Figure 6. Photocatalytic activity of the TiO_2 film deposited at 300 °C: (a) absorbance variation, (b) C_t/C_o degradation curve, (c) $-\ln(C_t/C_o)$ pseudo-first-order kinetic plot

After 540 min of UV-A irradiation, the film achieved 74% degradation, and the reaction rate constant was determined as k = 0.0025 min^{-1}. This value is approximately four times higher than that of the room–temperature film, indicating that the onset of crystallization at 300 °C is closely associated with the improved photocatalytic response. The weak but discernible anatase peaks observed in the XRD pattern of the 300 °C film suggest the early formation of a crystalline phase that is favourable for photocatalytic activity [24]. In addition, the granular surface morphology and increased roughness observed in the SEM and AFM analyses for the 300 °C film suggest a more developed film/solution interface, which may have contributed to improved MB degradation kinetics. As a result of these structural and surface enhancements, the TiO_2 film deposited at 300 °C exhibits significantly higher photocatalytic activity than the amorphous RT film.

On the other hand, the presence of Na diffusion from the soda–lime glass substrate into the TiO_2 film, as indicated by the SEM-EDX analysis, may act as a limiting factor for photocatalytic performance. Several studies have reported that Na ions diffusing from the glass substrate can suppress photoactivity by hindering anatase crystallization or promoting the formation of less photoactive phases [23,25]. In this context, Na incorporation observed in the 300 °C film may have partially restricted the potential photocatalytic enhancement despite the increased crystallinity. Nevertheless, the steady and stable degradation trend obtained in this study indicates that the photocatalytic process operated effectively under the applied experimental conditions.

4. Discussion

When the XRD, FTIR, SEM/AFM, and photocatalytic results are evaluated together, substrate temperature appears to be one of the main parameters governing the structural evolution and the resulting photocatalytic response of the sputtered TiO_2 films. The film deposited at room temperature remained XRD-amorphous, exhibited broad and weak Ti–O/Ti–O–Ti FTIR bands, showed a smooth and featureless surface morphology in SEM, and had a low RMS roughness of 4.306 nm. In contrast, the film deposited at 300 °C displayed weak but distinguishable anatase reflections, more clearly resolved Ti–O and Ti–O–Ti FTIR bands, a granular/columnar morphology, and a markedly higher RMS roughness of 26.03 nm. Taken together, these findings indicate that deposition at 300 °C initiates the earliest stage of structural ordering and surface development relative to room-temperature deposition [5,8,17].

The photocatalytic results directly reflect this structural evolution. While the room-temperature film exhibited only 26% MB degradation with a pseudo-first-order rate constant of 0.0006 min^{-1}, the film deposited at 300 °C reached 74% degradation with a rate constant of 0.0025 min^{-1}. Therefore, this enhancement should not be attributed to a single structural parameter, but rather to the combined effect of incipient anatase formation, a more organized Ti–O/Ti–O–Ti bonding structure, and temperature-induced surface development. In this context, the XRD results indicate the onset of crystallization, whereas the FTIR results support the formation of a more organized Ti–O/Ti–O–Ti network. Accordingly, the FTIR findings are interpreted here not as stand-alone proof of phase formation, but as complementary structural indicators supporting the transition toward a more photocatalytically favorable film structure [5,8,17].

The increase in surface roughness is also likely to have contributed to the enhanced photocatalytic activity. According to the AFM results, the RMS roughness increased from 4.306 nm to 26.03 nm, i.e., by nearly six times. This suggests a more developed film/solution interface, which may provide more accessible contact points for dye adsorption and surface reactions. In thin-

film photocatalysis, the literature reports that surface nano-texture and roughness can influence degradation kinetics through interfacial contact, adsorption behavior, and overall surface reactivity. However, roughness alone should not be considered a universal descriptor of activity, since its effect is strongly coupled with crystallinity, phase composition, and other microstructural factors. Therefore, in the present work, the higher roughness of the 300 °C film is interpreted as a contributing factor acting together with early anatase formation, rather than as the sole reason for the improved photocatalytic performance [10,26].

Another point that should be considered is the substrate–film interaction evidenced by SEM-EDX. The detection of Na, Si, Ca, and Mg, and particularly the semi-quantitative Na signal, indicates a non-negligible substrate/interfacial contribution within the analyzed volume. Because the TiO_2 layer is thin and the EDX interaction volume extends into the underlying soda–lime glass, the measured Na content should not be interpreted as the true depth-resolved Na distribution within the TiO_2 film. Nevertheless, the literature shows that sodium diffusing from soda–lime glass can alter the crystallization behavior of TiO_2-based coatings, promote less photoactive phases, and/or create recombination centers. The practical use of SiO_2 barrier layers to suppress Na migration further supports the relevance of this effect. Therefore, the Na signal detected in the present study is interpreted not as a fully quantified diffusion mechanism, but as evidence of a secondary factor that may have partially limited the photocatalytic enhancement achievable at 300 °C [8,27].

Overall, the present results indicate that deposition at a substrate temperature of 300 °C provides a favorable balance among early crystallization, Ti–O network ordering, surface development, and photocatalytic response without requiring a separate post-deposition annealing step. In this sense, the improvement observed at 300 °C supports the view that substrate temperature can be used as an effective processing parameter to enhance the performance of sputtered bare TiO2 thin films. A broader contextual comparison with selected sputtered TiO_2 thin-film studies is presented in Table 1.

As shown in Table 1, the photocatalytic performance obtained in the present study is competitive when compared with selected sputtered TiO_2 thin-film reports. Although some studies reported higher degradation efficiencies or higher rate constants, these differences are largely associated with variations in light source and power, pollutant type and initial concentration, substrate configuration, and additional processing steps such as post-deposition annealing or diffusion-barrier layers. Therefore, the values listed in Table 1 should be interpreted as contextual benchmarks rather than as a strict performance ranking. Within this framework, the 74% degradation efficiency and 2.50 × 10-3 min-1 rate constant obtained here, without any post-deposition annealing, represent a meaningful result for an undoped sputtered TiO_2 thin-film system.

Table 1. Comparison of photocatalytic degradation results reported for selected sputtered TiO_2 thin films

Preparation method / substrate	Deposition or post-treatment condition	Pollutant (initial concentration)	Light source	Time (min)	k (min^{-1})	Degradation (%)	Ref.
RF MS / glass	Substrate temperature: 200 °C	MB (5 mg L^{-1})	UV-A (365 nm, 64 W)	600	4.43×10^{-3}	82.0	[8]
Reactive RF MS / glass	Oxygen-rich deposition condition	MO (0.01 mmol L^{-1})	Xenon lamp (500 W, UV + visible)	80	NR	~70	[7]
DC MS / glass	250 nm SiO_2 barrier layer + 450 °C for 2 h	MB (2 µmol L^{-1})	UV-A (365 nm, 15 W)	60	1.04×10^{-3}*	5.8	[28]
DC MS of Ti layer / glass	Thermal oxidation at 550 °C	MB (10 mg L^{-1})	UV-A (40 W)	300	2.41×10^{-3}	53.51	[29]
RF MS / glass and Si	Deposited at room temperature	MO (5 ppm)	High-pressure mercury lamp (36 W)	180	3.69×10^{-3}	51.2	[30]
DC reactive MS / glass	Annealed at 500 °C	RhB (1×10^{-6} M)	Mercury lamp (200 W, 280–380 nm)	210	7.8×10^{-3}	80	[31]
RF MS / glass	**Deposited at 300 °C without post-deposition annealing**	**MB (2.5 mg L^{-1})**	UV-A (365 nm, 64 W)	**540**	**2.50×10^{-3}**	**74**	**This work**

Abbreviations: RF MS, Radio frequency magnetron sputtering; DC MS, Direct current magnetron sputtering; MB, methylene blue; MO, methyl orange; RhB, rhodamine B; NR, not reported.

Note: The k value in Ref. [28] was converted from s^{-1} to min^{-1} for consistency.

5. Conclusion

TiO_2 thin films deposited by RF magnetron sputtering at room temperature and at 300 °C were comparatively investigated in terms of structural, surface, and photocatalytic properties. The room-temperature film remained amorphous and showed limited photocatalytic activity, whereas the film deposited at 300 °C exhibited early crystallization, a more developed surface morphology, and higher surface roughness, resulting in significantly improved photocatalytic performance. The 300 °C film achieved 74% methylene blue degradation after 540 min and a higher apparent reaction rate than the room-temperature film. These results demonstrate that deposition at 300 °C is an effective condition for improving the photocatalytic response of sputtered TiO_2 thin films without a separate post-deposition annealing step. Overall, controlling the substrate temperature provides a simple and practical route to improve the structural and photocatalytic performance of bare sputtered TiO_2 thin films on low-cost soda–lime glass.

Conflicts of interest

There are no conflicts of interest in this work.

Acknowledgements

This work is supported by the Scientific Research Project Fund of Sivas Cumhuriyet University/Turkey under the project number **M-2021-806.**

References

[1] Miklos, D. B., Remy, C., Jekel, M., Linden, K. G., Drewes, J. E., & Hübner, U. (2018). Evaluation of advanced oxidation processes for water and wastewater treatment – A critical review. *Water Research*, 139, 118–131. https://doi.org/10.1016/j.watres.2018.03.042

[2] Tian, S., Feng, Y., Zheng, Z., & He, Z. (2023). TiO_2-Based photocatalytic coatings on glass substrates for environmental applications. *Coatings*, 13(8), 1472. https://doi.org/10.3390/coatings13081472

[3] Mulus, D. A. S., Permana, M. D., Deawati, Y., & Eddy, D. R. (2025). A current review of TiO_2 thin films: synthesis and modification effect to the mechanism and photocatalytic activity. *Applied Surface Science Advances*, 27, 100746. https://doi.org/10.1016/j.apsadv.2025.100746.

[4] Fujishima, A., & Honda, K. (1972). Electrochemical photolysis of water at a semiconductor electrode. *Nature*, 238(5358), 37–38. https://doi.org/10.1038/238037a0

[5] Wang, Y.-H., Rahman, K. H., Wu, C.-C., & Chen, K.-C. (2020). A review on the pathways of the improved structural characteristics and photocatalytic performance of titanium dioxide (TiO_2) thin films fabricated by the magnetron-sputtering technique. *Catalysts*, 10(6), 598. https://doi.org/10.3390/catal10060598

[6] Dell'Edera, M., Lo Porto, C., De Pasquale, I., Petronella, F., Curri, M. L., Agostiano, A., & Comparelli, R. (2021). Photocatalytic TiO_2-based coatings for environmental applications. *Catalysis Today*, 380, 62–83. https://doi.org/10.1016/j.cattod.2021.04.023.

[7] Ogawa, T., Zhao, Y., Okumura, H., & Ishihara, K. N. (2022). Enhanced photocatalytic activity of TiO_2 thin film deposited by reactive RF sputtering under oxygen-rich conditions. *Photochem*, 2(1), 138–149. https://doi.org/10.3390/photochem2010011

[8] Aydınoğlu, H. S.,& Şenadım Tüzemen, E. (2025). Effect of substrate temperature on the photocatalytic degradation efficiency of methylene blue using TiO_2 thin films. *Reaction Kinetics, Mechanisms and Catalysis*, 138, 3277–3294. https://doi.org/10.1007/s11144-025-02872-6

[9] Jana, S., Debnath, A. K., Putta, V., Bahadur, J., Kishor, J., Chauhan, A. K., & Bhattacharya, D. (2024). Effect of substrate temperature and annealing on the growth of TiO_{2-x} thin films deposited by using DC-magnetron sputtering technique. *Surface and Interface Analysis*, 56(2), 107–121. https://doi.org/10.1002/sia.7274

[10] Hosseini, Z. S., Haghparast, F., Masoudi, A. A., & Mortezaali, A. (2022). Enhanced visible photocatalytic performance of un-doped TiO_2 nanoparticles thin films through modifying the substrate surface roughness. *Materials Chemistry and Physics*, 279, 125530. https://doi.org/10.1016/j.matchemphys.2021.125530

[11] Szołdra, P., Frąc, M., Adamczyk, A., Kot, M., & Pichór, W. (2024). Characterization and photocatalytic activity of TiO_2 thin films prepared by sol-gel method for NOx degradation. *Materials Science and Engineering: B*, 301, 117189. https://doi.org/10.1016/j.mseb.2024.117189

[12] Grilli, M. L., Yilmaz, M., Aydogan, Ş., & Cirak, B. B. (2018). Room temperature deposition of XRD-amorphous TiO_2 thin films: Investigation of device performance as a function of temperature. *Ceramics International*, 44(10), 11582–11590. https://doi.org/10.1016/j.ceramint.2018.03.222

[13] Baqandwan, H., Mohamad Samsuri, S. A., Halim, M. M., & Pakhuruddin, M. Z. (2024). Nanostructured TiO_2 thin films sputtered at room temperature as electron transport layer for flexible perovskite solar cell applications: Impact of varying RF power. *Physica B: Condensed Matter*, 679, 415788. https://doi.org/10.1016/j.physb.2024.415788

[14] Mittireddi, R. T., Makani, N. H., Prajapati, D. G., Gautam, A. R. S., Banerjee, R., & Panda, E. (2023). Microstructure-induced functionality in titanium dioxide thin films. *Materials Characterization*, 199, 112818.https://doi.org/10.1016/j.matchar.2023.112818

[15] Hopoğlu, H., Aydınoğlu, H. S., Özer, A., & Şenadım Tüzemen, E. (2021). Investigation of nitrogen doped ZnO thin films: Effects on their structural and optical properties. *Optical Materials, 122*, 111685. https://doi.org/10.1016/j.optmat.2021.111685

[16] Güzelçimen, F., Tanören, B., Çetinkaya, Ç., Kaya, M. D., Efkere, H. İ., Özen, Y., Bingöl, D., Sirkeci, M., Kınacı, B., Ünlü, M. B., & Özçelik, S. (2020). The effect of thickness on surface structure of rf sputtered TiO_2 thin films by XPS, SEM/EDS, AFM and SAM. *Vacuum*, 182, 109766. https://doi.org/10.1016/j.vacuum.2020.109766

[17] Durante, O., Di Giorgio, C., Granata, V., Neilson, J., Fittipaldi, R., Vecchione, A., Carapella, G., Chiadini, F., DeSalvo, R., Dinelli, F., Fiumara, V., Pierro, V., Pinto, I. M., Principe, M., & Bobba, F. (2021). Emergence and evolution of crystallization in TiO_2 thin films: A structural and morphological study. *Nanomaterials*, 11(6), 1409. https://doi.org/10.3390/nano11061409

[18] Almeida, R. M., & Pantano, C. G. (1990). Structural investigation of silica gel films by infrared spectroscopy. *Journal of Applied Physics*, 68(8), 4225–4232. https://doi.org/10.1063/1.346213

[19] Khan, F. U., Zubair, M., Ansar, M. Z., Alamgir, M. K., & Nadeem, S. (2016). Effect of annealing temperature on the structural and optical properties of TiO_2 thin film prepared by sol-gel method. *Journal of Scientific Research*, 8(3), 267–272. https://doi.org/10.3329/jsr.v8i3.27195

[20] Igamov, B. D., Bekpulatov, I. R., Normamatov, A. M., Kamardin, A. I., Kodirova, F. S., & Imanova, G. (2026). Comprehensive analysis of thickness-dependent structural, morphological, and optical properties of TiO_2 based thin films. *Results in Optics*, 23, 100993. https://doi.org/10.1016/j.rio.2026.100993

[21] Mei, F., Yang, Z., Wu, L., Zhou, Y., & Zhang, D. (2012). Influence of annealing temperature on structure and photocatalytic activity of TiO_2 thin films prepared by DC reactive magnetron sputtering method. *Wuhan University Journal of Natural Sciences*, 17(4), 309–314. https://doi.org/10.1007/s11859-012-0847-y

[22] Escaliante, L. C., Rocha, K. O., & da Silva, J. H. D. (2021). Stability of the photocatalytic activity of TiO_2 deposited by reactive sputtering. *Materials Research*, 24(Suppl. 1), e20210051. https://doi.org/10.1590/1980-5373-MR-2021-0051

[23] Aubry, E., Ghazzal, M. N., Demange, V., Chaoui, N., Robert, D., & Billard, A. (2007). Poisoning prevention of TiO_2 photocatalyst coatings sputtered on soda–lime glass by intercalation of SiN_x diffusion barriers. *Surface and Coatings Technology*, 201(18), 7706–7712. https://doi.org/10.1016/j.surfcoat.2007.03.003

[24] Kéri, O., Kocsis, E., Karajz, D. A., Nagy, Z. K., Parditka, B., Erdélyi, Z., Szabó, A., Hernádi, K., & Szilágyi, I. M. (2021). Photocatalytic crystalline and amorphous TiO_2 nanotubes prepared by electrospinning and atomic layer deposition. *Molecules*, 26(19), 5917. https://doi.org/10.3390/molecules26195917

[25] Paz, Y., & Heller, A. (1997). Photo-oxidatively self-cleaning transparent titanium dioxide films on soda lime glass: The deleterious effect of sodium contamination and its prevention. *Journal of Materials Research*, 12(10), 2759–2766. https://doi.org/10.1557/JMR.1997.0367

[26] Khalifa, Z. S., Shaban, M., & Ahmed, I. A. (2023). Photocatalytic degradation of methyl orange and methylene blue dyes by engineering the surface nano-textures of TiO_2 thin films deposited at different temperatures via MOCVD. *Molecules*, 28(3), 1160. https://doi.org/10.3390/molecules28031160

[27] Chen, G.-S., Chen, J.-H., Kuo, J., & Niu, H. (2021). Highly crystallized mesoporous anatase films with enhanced photoactivity derived from sputter deposited TiO_2–WO_3 composites: The positive role of sodium. *Applied Surface Science*, 563, 150263. https://doi.org/10.1016/j.apsusc.2021.150263

[28] Villamayor, A., Pomone, T., Perero, S., Ferraris, M., Barrio, V. L., G-Berasategui, E., & Kelly, P. (2023). Development of photocatalytic nanostructured TiO_2 and NiO/TiO_2 coatings by DC magnetron sputtering for photocatalytic applications. *Ceramics International*, 49, 19309–19317. https://doi.org/10.1016/j.ceramint.2023.03.058

[29] Widyastuti, E., Chiu, C.-T., Hsu, J.-L., & Lee, Y.-C. (2023). Photocatalytic antimicrobial and photostability studies of TiO_2/ZnO thin films. *Arabian Journal of Chemistry*, 16, 105010. https://doi.org/10.1016/j.arabjc.2023.105010

[30] Meng, F., Cao, L., Song, X., & Sun, Z. (2009). Photocatalytic degradation of methyl orange by nano-TiO_2 thin films prepared by RF magnetron sputtering. *Chinese Optics Letters*, 7, 956–959. https://doi.org/10.3788/COL20090710.0956

[31] Tavares, C. J., Vieira, J., Rebouta, L., Hungerford, G., Coutinho, P., Teixeira, V., Carneiro, J. O., & Fernandes, A. J. (2007). Reactive sputtering deposition of photocatalytic TiO_2 thin films on glass substrates. *Materials Science and Engineering: B*, 138, 139–143. https://doi.org/10.1016/j.mseb.2005.11.043